

HARQ Optimization for Real-Time Remote Estimation in Wireless Networked Control

Faisal Nadeem, *Graduate Student Member, IEEE*, Yonghui Li, *Fellow, IEEE*, Branka Vucetic, *Life Fellow, IEEE*, Mahyar Shirvanimoghaddam, *Senior Member, IEEE*

Abstract—This paper analyzes wireless network control for remote estimation of linear time-invariant (LTI) dynamical systems under various Hybrid Automatic Repeat Request (HARQ) based packet retransmission schemes. In conventional HARQ, packet reliability increases gradually with additional packets; however, each retransmission maximally increases the Age of Information (AoI). A slight increase in AoI can cause severe degradation in mean squared error (MSE) performance. We optimize standard HARQ schemes by allowing partial retransmissions to increase the packet reliability gradually and limit the AoI growth. In incremental redundancy HARQ (IR-HARQ), we utilize a shorter time for retransmission, which improves the MSE performance by enabling the early arrival of fresh status updates. In Chase combining HARQ (CC-HARQ), since packet length remains fixed, we propose sending retransmission for an old update and new updates in a single time slot using non-orthogonal signaling. Non-orthogonal retransmissions increase the packet reliability without delaying the fresh updates. Using the Markov decision process formulation, we find the optimal policies of the proposed HARQ based schemes to optimize the MSE performance. We provide static and dynamic policy optimization techniques to improve the MSE performance. The simulation results show that the proposed schemes achieve better long-term average and packet-level MSE performance.

Index Terms—Age of Information, Finite block-length, HARQ, Remote estimation, Wireless networked control.

I. INTRODUCTION

The previous generation of cellular communications, such as third generation (3G) and fourth generation (4G), have primarily focused on increasing spectral efficiency for enhanced mobile broadband (eMBB) services [1]. The fifth generation (5G) mobile communication envisions to support real-time services, e.g., industrial automation, tactile internet, smart grid, telesurgery, virtual reality, etc. [2]. These services require very high reliability and low latency for in-time packet delivery. Most of these emerging mission-critical applications, for example, industrial automation and telesurgery, require remote estimation of the states of the underlying dynamic process over a wireless link [3]. Most of the existing work on remote estimation assumes a perfect channel and focuses on designing optimal control. However, the wireless channel can deteriorate the packet reliability leading to instability of the control system and unbounded error performance. Considering the nature of the application, communication, and control should be designed simultaneously [4].

The communication standards for eMBB services target average packet error rate (PER) reliability with little focus

on latency performance. However, in contemporary communication, designed to enable mission-critical applications that require remote estimation, the PER reliability is linked with its in-time packet delivery [5]. For example, in-time packet availability at the cost of less reliability could be more important than a reliable but outdated packet. The age-of-information (AoI) is an important performance metric to track the freshness of information defined as the measure of time elapsed between the moment a measurement is sent from the sensor and the moment it becomes available to the controller [6]. If the sensor always updates the remote-side controller with equal reliability, minimization of AoI leads to the lowest estimation error. This is usually the case when the dynamic process is highly uncorrelated between consecutive status updates. However, most of the time, the dynamic process to be controlled shows some correlation between its status updates [7], [8]. In this case, if a fresh status update does not arrive in time, the remote estimator can estimate the new status from previously received status updates. Furthermore, in a real-time remote estimation of a correlated dynamic process, a fine balance between reliability and freshness should be maintained [9]. For example, when the system is slowly evolving, a more reliable old update can better estimate the next state than a less reliable fresh update. In these situations, many researchers suggest performance metrics that are non-linear in terms of AoI, such as the value of information and estimation mean squared error (MSE) [9]–[11].

To vary the reliability of different updates of the system, many authors question the usefulness of the packet retransmission schemes with feedback, such as automatic repeat request (ARQ) [12], [13]. For example, when the controller has no knowledge of the system correlation, and it cannot estimate the new update from previous status updates at all, then the standard ARQ is the optimal scheme [12]. In the standard ARQ protocol, the sensor always sends the latest available update, and if the packet fails, the receiver discards that packet altogether. However, hybrid automatic repeat request (HARQ) utilizes forward error correction coding to facilitate combining the failing packet with its retransmissions to increase the reliability of an estimate [14], [15]. Given some knowledge of the dynamic process, the policy of sending new or retransmitting old updates is used to minimize the average MSE performance of such systems [11]. When a packet is successful with HARQ, the feedback acknowledgment (ACK) signal requests the sensor to send a fresh update; otherwise, it repeats the old status update when a negative ACK (NACK) is received. HARQ has two common types: Chase combining HARQ (CC-HARQ) and incremental redundancy HARQ (IR-HARQ). In CC-HARQ, the whole packet is repeated, and by utilizing maximum ratio combining (MRC) at the receiver, the reliability is increased.

The authors are with the Centre for IoT and Telecommunications, School of Electrical and Information Engineering, The University of Sydney, NSW 2006, Australia. Emails: {faisal.nadeem, yonghui.li, branka.vucetic, mahyar.shm}@sydney.edu.au.

With IR-HARQ, the transmitter increases code redundancy by sending a long codeword in chunks, and the receiver improves reliability by improving the decoding performance with a longer codeword after each retransmission [16]. HARQ increases reliability at the expense of increased latency to fresh updates with each retransmission. Therefore, in the latest specifications of 5G for low-latency communication, only 1 or 2 retransmissions is supported [17]. Both IR-HARQ and CC-HARQ are studied in the finite blocklength (FBL) regime for their effectiveness in low-latency communication [15], [18]. HARQ is also optimized to meet strict packet-level latency requirements in Rayleigh fading channel [19], [20]. Most of the work on HARQ based remote estimation only focuses on sending a new update or an old update by optimal action in each time slot. However, little focus has been given to improving HARQ performance for such a system.

In this paper, we optimize the performance of HARQ based real-time remote estimation systems and optimally design the sensor's transmission policy to minimize the estimation MSE. The proposed HARQ protocols utilize the fundamental trade-off between the reliability and freshness of the sensor's measurement with greater flexibility than standard HARQ. For IR-HARQ, we optimize the retransmissions packet lengths to limit the MSE and get more stability in MSE performance. We improve the standard CC-HARQ for wireless remote estimation. In standard CC-HARQ, the sensor has only two choices at any available time slot, i.e., repeat an entire packet of old updates or send fresh updates instead. This limit of choices leads to poor MSE performance. We choose the right combination of new and old updates using non-orthogonal signaling and found the optimal policy using the Markov decision process (MDP). The proposed non-orthogonal CC-HARQ (N-CC-HARQ) based remote estimation achieves minimum and more stable MSE performance than standard CC-HARQ. We also enhance the N-CC-HARQ scheme by varying non-orthogonal combinations of fresh and old updates among various time slots and obtain optimal policies named as static and dynamic policies for N-CC-HARQ. The main contributions of the paper are summarized as follows:

- We optimize the IR-HARQ and CC-HARQ based packet retransmission schemes for providing better MSE performance for a real-time remote estimation system. In IR-HARQ, we optimize the retransmission fraction according to the varying correlation of the underlying dynamic process. Optimal retransmissions enable quicker status updates, limit AoI growth, and improve the MSE performance. The underlying policy optimization problem is complex, so we provide a detailed MDP framework to obtain the optimal policy iteratively using numerical techniques.
- We propose N-CC-HARQ to implement incremental age and reliability growth. N-CC-HARQ uses superposition coding with power fraction $0 \leq \alpha \leq 1$ to support simultaneous transmission of fresh update and retransmission of an old status update in a single time slot. We further formulate an MDP-based optimization problem, where best α is chosen to reduce average estimation MSE and

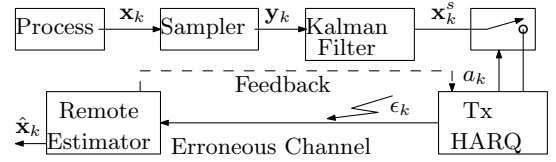


Fig. 1. The system model for remote estimation of a dynamic process using HARQ over a wireless channel

provide more stable MSE performance.

- Next, we show the impact of α on the system performance, present a static and dynamic setting of α , and find the optimal policy. In a static-optimal policy, the optimal α remains fixed for all time slots. The static-optimal policy using N-CC-HARQ achieves better MSE performance than the optimal policy with standard CC-HARQ. We further enhance the N-CC-HARQ performance by designing a dynamic-optimal policy. With a dynamic-optimal policy, the sensor can select a non-orthogonal power fraction α in each time slot. The dynamic action increases flexibility and leads to better MSE performance than static-optimal policy.
- Simulation results show that optimal policies under proposed HARQ schemes achieve much higher performance gain over standard HARQ based optimal policies. The simulations also compare the MSE performance for higher-order statistics, which show a stability performance guarantee of the proposed design and the average MSE performance improvements.

The rest of the paper is organized as follows. The system model and preliminaries on wireless remote estimation of linear time invariant (LTI) system with HARQ in the FBL regime and general problem formulation are presented in Section II. In Section III, we present a detailed analysis of proposed IR-HARQ and CC-HARQ based schemes using MDP. We provide numerical results in Section IV, where we compare IR-HARQ and CC-HARQ for long-term average MSE and its packet-level distribution. Finally, Section VI concludes the paper.

II. SYSTEM MODEL AND PRELIMINARIES

Similar to [11], we assume that a smart sensor periodically samples the dynamic process, performs local estimates using the Kalman filtering, and sends the local estimates over the wireless links. As illustrated in Figure 1, the sensor utilizes retransmission using HARQ to increase reliability.

A. Dynamic Process Modeling

We model the dynamical process with a general discrete LTI system to be estimated remotely given as (e.g., [21], [22])

$$\begin{aligned} \mathbf{x}_{k+1} &= \mathbf{A}\mathbf{x}_k + \mathbf{w}_k, \\ \mathbf{y}_k &= \mathbf{C}\mathbf{x}_k + \mathbf{v}_k, \end{aligned} \quad (1)$$

where the sampling period of the sensor T_s determines the discrete time steps denoted by index k . Vector $\mathbf{x}_k \in \mathbb{R}^n$ contains the states of the dynamic process that varies according to state transition matrix $\mathbf{A} \in \mathbb{R}^{n \times n}$. The sampler collects m measurements denoted as $\mathbf{y}_k \in \mathbb{R}^m$ according to measurement matrix $\mathbf{C} \in \mathbb{R}^{m \times n}$ for local state estimation as shown in Fig.

1. The $\mathbf{w}_k \in \mathbb{R}^n$ and $\mathbf{v}_k \in \mathbb{R}^m$ are identically distributed (i.i.d.) zero-mean Gaussian processes and measurement noise vectors with corresponding covariance matrices \mathbf{Q}_w and \mathbf{Q}_v respectively. The initial state \mathbf{x}_0 is zero-mean Gaussian with covariance matrix Σ_0 . We assume that the maximum squared eigenvalue of \mathbf{A} is greater than 1 to avoid trivial problem [23].

B. Local State Estimation

The sensor collects raw measurements that are noisy. However, with some storage and computation, a sensor can process the raw data to get state estimation of a process \mathbf{x}_k . This can be done using the state-of-the-art Kalman filter [22] to get minimum MSE in state estimation from current and previous raw measurements as follows:

$$\mathbf{x}_{k|k-1}^s = \mathbf{A}\mathbf{x}_{k-1|k-1}^s \quad (2a)$$

$$\mathbf{P}_{k|k-1}^s = \mathbf{A}\mathbf{P}_{k-1|k-1}^s \mathbf{A}^T + \mathbf{Q}_w \quad (2b)$$

$$\mathbf{K}_k = \mathbf{P}_{k|k-1}^s \mathbf{C}^T (\mathbf{C}\mathbf{P}_{k|k-1}^s \mathbf{C}^T + \mathbf{Q}_v)^{-1} \quad (2c)$$

$$\mathbf{x}_{k|k}^s = \mathbf{x}_{k|k-1}^s + \mathbf{K}_k (\mathbf{y}_k - \mathbf{C}\mathbf{x}_{k|k-1}^s) \quad (2d)$$

$$\mathbf{P}_{k|k}^s = (\mathbf{I} - \mathbf{K}_k \mathbf{C}) \mathbf{P}_{k|k-1}^s, \quad (2e)$$

where at time k , $\mathbf{x}_{k|k-1}^s$ and $\mathbf{x}_{k|k}^s$ denotes the *priori* and *posteriori* state estimates, respectively, whereas, $\mathbf{P}_{k|k-1}^s$ and $\mathbf{P}_{k|k}^s$ are the *priori* and *posteriori* error covariance matrices, respectively. With the Kalman gain, \mathbf{K}_k , first two equations are used to perform prediction, whereas rest are used to update the estimates [24]. It is important to note that remote estimation is worse than local estimation due to involved additional channel uncertainties, etc. Also, local estimation should be stable in order to achieve stabilized remote estimation. We assume that parameters (\mathbf{A}, \mathbf{C}) of the LTI system in (1) are observable while parameters $(\mathbf{A}, \sqrt{\mathbf{Q}_w})$ are reachable. This guarantees the stability of the local estimation for a sufficiently large k , such that $\mathbf{P}_{k|k}^s = \mathbf{P}_0$ [25], where \mathbf{P}_0 represent the converged error covariance matrix.

C. Channel Model

Let $s(t)$ and $y(t)$, denote the transmitted and received signal, at time t , respectively. Then, $y(t)$ is given by:

$$y(t) = s(t) + w(t), \quad (3)$$

where $w(t) \sim \mathcal{CN}(0, N_0)$ is the circularly symmetric zero-mean complex additive white Gaussian noise (AWGN). We also assume that the total transmit power is $\mathbb{E}[|s(t)|^2] = P_t$ and $s(t)$ is linearly modulated and transmitted with normalized symbol rate 1 symbol/s/Hz. Note that we assume $N_0 = 1$. Each information packet of k message bits is encoded into a codeword of length n and transmitted using HARQ in m retransmission rounds. We further assume perfect ACK/NACK signaling, where each feedback is being received instantly and without error.

D. HARQ-based Communication over AWGN channel

The sensor's local estimation is first quantized into k message bits and encoded into a packet carrying n symbols, each taking T_s' duration. The sampling period of the sensor

is set to be $T_s = nT_s'$ so that the sensor continuously samples at a single packet duration. Therefore, a new sample update is collected after delivering one packet of duration nT_s' . In each time slot, the sensor can take action $a_k = 0$ to send a fresh update or $a_k = 1$ to repeat the old update. In ARQ, the receiver always decodes with a fixed level of reliability irrespective of the sensor action a_k . However, the sensor can utilize the HARQ to improve the reliability of an update with action $a_k = 1$. In HARQ, the sensor sends a coded packet in multiple time slots, and the decoder can combine the repeated transmissions to improve packet reliability.

HARQ improves packet reliability with each retransmission in two different ways, i.e., incremental signal-to-noise-ratio (SNR) or incremental redundancy known as CC-HARQ and IR-HARQ, respectively. In CC-HARQ, the full coded packet of length n is repeated for retransmission purposes and combined with MRC followed by decoding decision. In CC-HARQ, the codeword length n remains fixed, while the effective SNR improves with each retransmission. In IR-HARQ, the transmitter encodes packets using a longer (n, k) channel code and initially sends n_1 symbols of the codeword with action $a_k = 0$. If the packet reliability is not satisfactory with $a_k = 0$, the transmitter attempts to improve the reliability by tacking action of retransmission, i.e., $a_k = 1$. IR-HARQ based transmitter sends additional $n_2 = \tau n$ symbols of the codewords against action $a_k = 1$. With each action $a_k = 1$, more redundancy is released, until the transmitter sends new packets with the action $a_k = 0$ or maximum n symbols are sent. IR-HARQ increases the codeword length with each retransmission, thus increasing the robustness of the error correction performance with longer codewords.

We assume that the sensor utilizes short packets to send each update. Using normal approximation [26], the error rate in the FBL can be characterized¹. The error rate with m cumulative transmissions of CC-HARQ and IR-HARQ can be written, respectively, as [28], [29]

$$\epsilon_{cc}([\gamma_i]_1^m) \approx Q\left(\frac{n \log_2(1 + \sum_{i=1}^m \gamma_i) - k + \log_2(n)}{n \sqrt{V(\sum_{i=1}^m \gamma_i)}}\right), \quad (4)$$

$$\epsilon_{ir}([\gamma_i]_1^m, [n_i]_1^m) \approx Q\left(\frac{\sum_{i=1}^m n_i \log_2(1 + \gamma_i) - k + \log_2(\sum_{i=1}^m n_i)}{\sqrt{\sum_{i=1}^m n_i V(\gamma_i)}}\right), \quad (5)$$

where $[x]_1^m = [x_1, \dots, x_m]$, $V(\gamma_i) = \left(1 - (1 + \gamma_i)^{-2}\right) \log_2^2(e)$ is the channel dispersion, γ_i is the SNR at the i -th transmission round, and $Q(\cdot)$ is the standard Q -function.

E. Remote State Estimation

We assume that the sensor continuously updates the receiver by sending packets in each time slot. If a packet fails in the

¹This bound was also used in [27] to analyze the performance of HARQ schemes and verified using practical LT codes.

current time slot, the receiver estimates the state based on the old successful packets in the most immediate previous time slots. However, a current state estimate based on the old update leads to poor estimation due to higher AoI. We assume that one unit packet transmission delay is equivalent to a unit time slot that exists between receiver and the sensor. Thus a sensor's measurement at time slot k is available to the receiver before time slot $k+1$. If the packet fails, it delays the estimation by unit time slot, i.e., AoI increases by one. More specifically, if the sensor's local estimate generated at the time instant t_k , denoted as $\hat{\mathbf{x}}_{t_k}^s$, becomes available to the receiver at the beginning of time slot k , the q_k is given as [30]

$$q_k = k - t_k, \quad \forall k \quad (6)$$

where $q_k \geq 1$ is the AoI. The receiver estimation quality depends upon the AoI. With AoI measure q_k , the optimal MSE estimator at the receiver at the beginning of time slot k is [21]

$$\hat{\mathbf{x}}_k = \mathbf{A}^{q_k} \hat{\mathbf{x}}_{t_k}^s, \quad (7)$$

and the error covariance matrix of the estimation can be defined as [21]

$$\mathbf{P}_k = \mathbb{E}[(\mathbf{x}_k - \hat{\mathbf{x}}_k)(\mathbf{x}_k - \hat{\mathbf{x}}_k)^T], \quad (8)$$

then putting (1) and (7) into (8), the one-to-one correspondence of remote estimation error covariance with the AoI q_k is obtained as

$$\mathbf{P}_k = f^{q_k}(\bar{\mathbf{P}}_0), \quad (9)$$

where $f(\mathbf{X}) \triangleq \mathbf{A}\mathbf{X}\mathbf{A}^T + \mathbf{Q}_w$ and $f^{\ell+1}(\cdot) \triangleq f(f^\ell(\cdot))$ $f^1(\cdot) \triangleq f(\cdot)$. Then, the instantaneous cost associated with the remote estimation error is $\text{Tr}(\mathbf{P}_k)$. According to [23, Lemma 3.1] $\text{Tr}(\mathbf{P}_k)$ monotonically increases with q_k , i.e., $\text{Tr}(f^{\ell_1}(\bar{\mathbf{P}}_0)) \leq \text{Tr}(f^{\ell_2}(\bar{\mathbf{P}}_0))$, $\ell_2 \geq \ell_1 \geq 1$ [31]. The MSE estimation quality also depends upon the dynamics of the process. If the correlation of the process is lower, then the receiver can estimate the process upon failing a packet with less error. On the other hand, if the status change of the LTI process is faster, the MSE estimation penalty is higher with the AoI. The maximum squared eigenvalue of the process state matrix $\rho^2(\mathbf{A})$ indicates the correlation of the process. A higher $\rho^2(\mathbf{A})$ shows a low correlation among consecutive states of the LTI process

F. Performance metrics and Problem Formulation

In each time slot, the sensor can take action $a_k \in \mathcal{A}$, where $\mathcal{A} \in \{0, 1\}$ for standard HARQ [11]. The long-term average MSE performance denoted as $\bar{\mu}_{\text{MSE}}$ over K time slots is due to the sequence of actions $\{a_1, a_2, \dots, a_k, \dots\}$ by the sensor, where a_k is the action taken at the k -th time slot.

$$\bar{\mu}_{\text{MSE}} = \limsup_{K \rightarrow \infty} \frac{1}{K} \sum_{k=1}^K \mathbb{E}[\text{Tr}(\mathbf{P}_k)] \quad (10)$$

where $\limsup_{K \rightarrow \infty}$ is the limit superior operator. Then, the sensor policies are action sequences during the process control, leading to a specific long-term average MSE cost. Then, the first objective is to find the optimal policy so that the long-term average estimation error is minimized,

The long-term average MSE provides a mean performance guarantee over many time slots. However, in the critical remote estimation for process control, the higher-order moments such as standard deviation from the mean of the MSE are also important performance metrics. A system that offers less deviation from the mean in each time slot provides higher stability in maintaining the target performance. The expected standard deviation to the average MSE is defined as follows

$$\rho_{\text{MSE}} = \mathbb{E}[(\text{Tr}(\mathbf{P}_k) - \mathbb{E}[\text{Tr}(\mathbf{P}_k)])^2]. \quad (11)$$

The second objective is to minimize the standard deviation. Then, the optimal policy is to find the sequence of proper actions such that long-term average MSE and the standard deviation are minimized. The dual objective optimization problem is defined as

$$\text{Prob}_1 : \min_{\{a_1, a_2, \dots, a_k, \dots\} \forall a_k \in \mathcal{A}} \{\bar{\mu}_{\text{MSE}}, \rho_{\text{MSE}}\}, \quad (12)$$

The above problem is very complex due to the intractable analytical form of the multi-objective function, and the analytical solution to the above problem is not realizable. We adopt a step-by-step procedure to achieve the target objective, summarized as follows. Firstly, it can be seen that problem **Prob**₁ can be transformed into two discrete problems, each targeting the individual objective. Secondly, to find the optimal policy so that each targeted objective is met, we break the problem into two parts, i.e., designing the action space \mathcal{A} and finding the best sequence of actions. To minimize the above objective over a set of actions, we modify the action space offered by standard HARQ schemes, i.e., two discrete choices $a \in \{0, 1\}$ in each time slot corresponding to a specific increment to AoI. We try to minimize the AoI with retransmission by proposing more flexible HARQ schemes such that after the retransmission, the AoI growth is limited. For example, the action set using IR-HARQ would also include the amount of redundancy for each retransmission. Similarly, under N-CC-HARQ, the sensor would have various power fraction α choices to conduct retransmission. Then, to solve **Prob**₁, the best policy can be obtained iteratively using the MDP framework. Next, we provide a detailed analysis of each HARQ scheme and its MDP formulation to get the optimal solution to the problem.

III. ANALYSIS AND OPTIMIZATION OF TRANSMISSION CONTROL WITH HARQ

In this section, we focus on developing HARQ based strategies that lead to various policies while meeting the objectives of problem **Prob**₁. IR HARQ and CC-HARQ types of HARQ schemes are optimized by modifying the action space such that the AoI growth with retransmission is controlled. The MDP formulation is utilized to obtain the optimal policies for various proposed HARQ schemes.

A. IR-HARQ based scheme

1) *Transmission control policy with $0 \leq \tau \leq 1$* : As show in Fig. 2, the action taken at each time slot is denoted as $a \in \{0, 1\}$. The k -th time slot duration is given as $T_{k-1}T_k$.

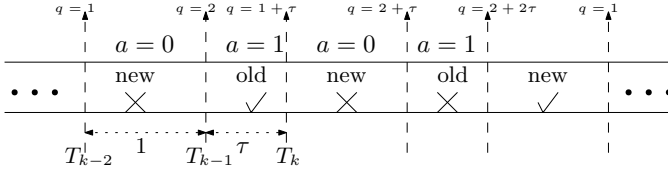


Fig. 2. The packets transmission model with IR-HARQ when maximum single retransmission of a failing status update is enabled utilizing τ fraction of the unit time slot

During the time slot $k-1$ the sensor updates the controller with the fresh update with the action $a = 0$. The receiver is unable to decode the packet, and sensor sends the next packet of length τ related to the old update in time slot k with action $a = 1$. Note that the time slot duration is 1 and τ for action $a = 0$ and $a = 1$ respectively. The shorter time slot utilization $\tau < 1$ leads to marginal reliability improvement with less packet arrival delay in comparison to $\tau = 1$. Note that in Fig. 2, we allow maximum single retransmission. If the packet fails after maximum retransmissions, the transmitter sends a fresh update in the next time slot. We assume that the sensor and remote receiver are perfectly synchronized. For the system with m retransmissions the AoI growth q_k due to action of the sensor a_k according to the packet success and failing indicator ζ_k can be written as

$$q_k = \begin{cases} 1, & a_{k-1} = 0, \zeta_{k-1} = 0, \\ q_{k-1} + 1, & a_{k-1} = 0, \zeta_{k-1} = 1, \\ (m_{k-1} - 1)\tau + 1, & a_{k-1} = 1, \zeta_{k-1} = 0, \\ q_{k-1} + (m_{k-1} - 1)\tau + 1, & a_{k-1} = 1, \zeta_{k-1} = 1, \end{cases} \quad (13)$$

where m_{k-1} denotes the number of consecutive transmissions for single status update until time slot $k-1$, $\zeta_k = 0$ and $\zeta_k = 1$ indicates the packet successful and fail states at the receiver during time slot k , respectively. The packet reliability for IR-HARQ at various m can be obtained in (5). The error covariance between discrete age points of (9) can be approximated by the help of curve fitting and proper scaling to model the MSE due to shorter time slots (τ) utilization during the retransmissions.

2) *Problem Formulation*: For a given τ , the sensor can act to send a fresh update or retransmission of an old update in each time slot. The sensors control policy is the sequence of actions over many time slots, leading to specific long-term average estimation error performance. The goal is to find the optimal policy and τ such that long-term estimation MSE is minimized. Furthermore, to ensure the stable and bounded error performance in each time slot, the standard deviation of error is also minimized. The optimization problem can be written as

$$\min_{\tau} \left\{ \min_{\lambda(\tau)} \{ \bar{\mu}_{\text{MSE}}, \rho_{\text{MSE}} \} \right\}, \quad (14)$$

where $0 \leq \tau \leq 1$, $\bar{\mu}_{\text{MSE}}$ and ρ_{MSE} are long-term average MSE and its standard deviation given in (10) and (11), respectively.

The analytical solution of (14) for online decision is intractable. For a discrete τ , the objective functions of (14) depend on the estimation error and action of the sensor in each time slot. The estimation error is a non-linear function of AoI according to (9). Also, for a fixed τ , according to (13), the AoI

q_k in time slot k depends on the action a_{k-1} and retransmission count m_{k-1} in the previous time slot. Therefore, the problem can be defined as a discrete-time MDP, and optimal policy can be obtained using numerical techniques.

3) *MDP Formulation*: In general, an MDP is defined by state space, action space, state transition function and reward function (cost function) denoted as \mathbb{J} , \mathbb{A} , $\mathbb{P}(J_k|J_{k-1}, a)$ and $\mathbb{C}(J_k, a)$, respectively, where $J_k \in \mathbb{J}$ is the state at time k . The components are defined as follows

1) **The state space** is $\mathbb{J} \triangleq \{(m, q), \in N \times N\}$, such that $J_k \triangleq (m_k, q_k) \in \mathbb{J}$ denotes the state of the MDP at time k . We assume that τ is fixed for a static policy and do not vary across time slots².

2) **The action space** of the MDP is $\mathbb{A} \triangleq \{0, 1\}$, where action $a = 0$ corresponds to the sensor sending a fresh update using length n_1 packet. The action $a = 1$ corresponds to the sensor retransmitting an old update with packet length $n_2 = \tau n_1$, where $0 \leq \tau \leq 1$. Selecting higher τ increases packet reliability at the cost of a rapid increase in AoI (q) with each retransmission.

3) **The state transition function** $\mathbb{P}(J_n|J_c, a)$ is the probability of state transition from current state J_c to the next state J_n with action set \mathbb{A} . When the sensor takes action $a = 0$, the fresh update is transmitted, i.e., $m = 1$. With each retransmission action $a = 1$, m increases by single unit. Therefore, the state transition function for IR-HARQ with partial retransmissions of τ units is given as

$$\mathbb{P}(J_n|J_c, a) = \begin{cases} 1 - \epsilon_{\text{ir}}^{(m)}, & J_n = (m, (m-1)\tau + 1), \\ \epsilon_{\text{ir}}^{(m)}, & J_n = (m, q + (m-1)\tau + 1), \\ 0, & \text{otherwise,} \end{cases} \quad (15)$$

where, during action $a = 0$ and $a = 1$, $m = 1$ and $m > 1$ respectively. We drop the time index k because the state transition function is time-homogeneous. Also in (15), $\epsilon_{\text{ir}}^{(m)}$ is the concise notation corresponding to the error probability of IR-HARQ in finite block length at the m -th transmission given in (5) as $\epsilon_{\text{ir}}([\gamma_i]_1^m, [n_i]_1^m)$.

4) **The cost function** associated with each action is the instantaneous MSE at the current state. The cost function is a non-linear function of AoI q given as

$$\mathbb{C}(J_n, a) \triangleq \text{Tr}(f^q(\bar{\mathbf{P}}_0)). \quad (16)$$

Under sufficient condition [11, Theorem 1], we assume that stationary and deterministic policy $\lambda(\tau)$ exists that guarantees bounded long-term average MSE cost. Therefore, at a given τ , problem (14) is equivalent to the MDP average cost optimization problem. Provided that sufficient condition holds, the MDP problem can be solved using relative value iteration or policy iteration algorithms [32]. The optimal policies corresponding to each discrete value of τ can be compared to get the best $\lambda(\tau)$. This step is shown as outer optimization in problem (14).

Remark 1. The equivalent MDP problem of [11, Eq.(25)] can be obtained by fixing maximum retransmissions to 1 and $\tau = 1$

²The flexibility of varying τ in each time slot can further optimize the performance at the cost of complexity. However, we provide the dynamic setting under CC-HARQ only, for simplicity of presentation

in (15). Therefore, the IR-HARQ based approach adopted in [11] is a special case of the above proposed design when $\mathbb{A} \triangleq \{0, 1\}$ and $\tau_1 = 1$. We refer to it as standard IR-HARQ design in this work. A rather more similar work that recently published [33] tried to find the optimal policy when the sensor can take the action of sending different lengths of packets. This is because when the packet length increase, the reliability also increases. However, the author in [33] did not consider the HARQ scheme, which increases the reliability due to erroneous decoding of subsequent packets, but various packet lengths are allowed in the actions space to the sensor. Therefore, it is fundamentally different than the approach we adapted for IR-HARQ in this paper.

B. Standard CC-HARQ

The standard CC-HARQ based optimal policy can be obtained using the MDP formulation for IR-HARQ by modifying the transition function (15) with the error probability ϵ_{cc} of CC-HARQ given in (4) and keeping $\tau = 1$. In standard CC-HARQ, the full packet is repeated in response to retransmission requests, and the receiver increases the reliability using MRC. The MSE error performance of the optimal policy with IR-HARQ at $\tau = 1$ is better than standard CC-HARQ based optimal policy at a given SNR, and rate [11]. However, CC-HARQ is also an important candidate for mission-critical application due to its fixed packet structure and simple receiver design. We optimize the CC-HARQ strategy to minimize the achievable MSE performance in the subsequent sections.

C. Proposed non-orthogonal CC-HARQ scheme

In standard CC-HARQ, time slots for sending the new transmission and retransmission are fixed due to its packet combining based decoding. The sensor's retransmissions occupy the full available time slot to send old estimates. However, the time taken by each action causes the AoI to increment accordingly. Therefore, the standard CC-HARQ offers little flexibility in the choice of reliability and AoI growth with action $a = 1$. We propose a non-orthogonal CC-HARQ scheme. The sensor can send the old update as retransmission non-orthogonally, using the power-sharing fraction α with a fresh update. More specifically, during retransmission, the sensor superimposes the previous and current updates with power fractions αP and $(1-\alpha)P$. So that the receiver combines the retransmission with the old available packet using MRC and decodes it under the interference of the fresh update. After removing the old packet using successive interference cancellation (SIC), the receiver can recover the fresh update for decoding. In this way, two different reliability and AoI options would be available to the decoder in a single time slot of retransmission. This provides the receiver greater flexibility of packet reliability and age with action $a = 1$ as can be seen in Fig. 3(b). Whereas, Fig. 3(a) indicates that in the standard CC-HARQ, every time retransmission is conducted, the AoI is maximally increased.

1) *Transmission control for N-CC-HARQ with α* : As shown in Fig. 3(b), N-CC-HARQ follows a similar time slot structure as standard CC-HARQ. For each time slot, the sensor is allowed to take action $a \in \{0, 1\}$. The sensor sends the fresh

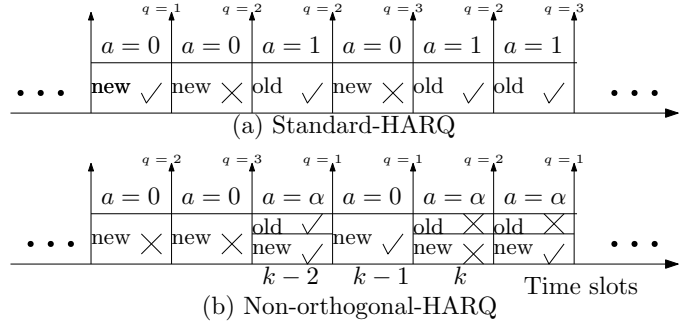


Fig. 3. The packet transmission structure with AoI due to standard CC-HARQ and N-CC-HARQ with a single retransmission

update with full power P occupying a unit time slot. If the packet with the fresh update fails with action $a = 0$, the receiver estimates the current state from an old update with higher AoI. As shown in Fig. 3, the consecutive packet failure causes AoI to grow significantly, resulting in higher MSE. Retransmission can increase the packet reliability with a single unit increase in AoI q . With N-CC-HARQ due to $a = 1$, if the old packet is successfully recovered but the overlapping fresh packet fails, the AoI increases by 1. However, if the non-orthogonal fresh update is also successfully decoded with $a = 1$, AoI would be 1. The AoI update rule for N-CC-HARQ due to packet success and failure when maximum single retransmission is allowed, i.e., $m = 2$, is given as follows:

$$q_k = \begin{cases} 1, & a_{k-1} = 0, \zeta_{k-1} = 0, \\ 1, & a_{k-1} = 1, \zeta_{k-1}^o = 0, \& \zeta_{k-1}^c = 0, \\ 2, & a_{k-1} = 1, \zeta_{k-1}^o = 0 \& \zeta_{k-1}^c = 1, \\ q_{k-1} + 1, & \zeta_{k-1} = 1 \text{ or } \zeta_{k-1}^o = 1, \end{cases} \quad (17)$$

where $\zeta_{k-1} = 0$ and $\zeta_{k-1} = 1$ indicate the packet success or fail state at the decoder when the sensor takes action $a = 0$. ζ_{k-1}^o and ζ_{k-1}^c indicate packet fail or success states corresponding to old update and fresh (current) update, respectively, with action $a = 1$. With HARQ in the static channel, the packet with more retransmission has better reliability than a packet with less retransmission. Therefore, we assume if decoding of an old update fails after retransmission, its non-orthogonally overlapping fresh update also fails and requires retransmission. Parameter α can be tuned to achieve the required reliability with a marginal AoI increment in a time slot.

2) *Problem formulation*: The control policy of the sensor with proper α results in minimizing the long-term average MSE and provides MSE stability per time slot. Similar to the IR-HARQ based policy optimization problem with τ in (14), the structure of the policy optimization problem for N-CC-HARQ with α is given as follows:

$$\min_{\alpha} \left\{ \min_{\lambda(\alpha)} \{ \bar{\mu}_{\text{MSE}}, \rho_{\text{MSE}} \} \right\}, \quad (18)$$

where $0 \leq \alpha \leq 1$. Problem (18) is highly complex, and its on-line analytical solution is difficult to obtain. Following similar treatment as with (14), we can obtain a numerical solution by solving the equivalent MDP problem using iterative methods. Next, we provide details of MDP.

3) *MDP Problem formulation*: Similar to the MDP of standard IR-HARQ given in Section III-A, the MDP formulation with state of m_k and q_k can be obtained for N-CC-HARQ. The underlying MDP can be defined using the state at time k according to reliability metric m and AoI q . The state space is $\mathbb{J} \triangleq \{(m, q) \in N \times N\}$, where $J_k \triangleq (m_k, q_k) \in \mathbb{J}$ is the state at k -th time slot. The action space $\mathbb{A} \triangleq \{0, 1\}$ is defined by the action $a = 0$ and $a = 1$, where action $a = 1$ corresponds to the action of non-orthogonal retransmission with power sharing between old and fresh update with fraction $0 \leq \alpha \leq 1$.

Lemma 1. *The state transition function $\mathbb{P}(J_n|J_c, a)$ for N-CC-HARQ for the system with single retransmission and power-sharing fraction $0 \leq \alpha \leq 1$ between fresh and old update when $a = 0$ is given by*

$$\mathbb{P}_\ell(J_n|J_c, a) = \begin{cases} 1 - \epsilon(\gamma_1); & J_n = (1, 1), \\ \epsilon(\gamma_1); & J_n = (1, q + 1), \end{cases}$$

and when $a = 1$, is given by

$$\mathbb{P}_\ell(J_n|J_c, a) = \begin{cases} (1 - \epsilon(\gamma_i, \gamma_I))(1 - \epsilon(\gamma_2)); & J_n = (1, 1), \\ (1 - \epsilon(\gamma_i, \gamma_I))\epsilon(\gamma_2); & J_n = (2, 2), \\ \epsilon(\gamma_i, \gamma_I); & J_n = (2, q + 1), \\ 0; & \text{else,} \end{cases}$$

where $\gamma_1 = P$, $\gamma_2 = (1 - \alpha)P$, and $\gamma_I = \frac{\alpha P}{1 + (1 - \alpha)P}$.

Proof: The state transition probabilities regarding action $a = 0$ are trivial. When the sensor takes action $a = 1$ with a specific α , the receiver can recover the fresh update from the overlapping packet at $q = 1$ with probability $(1 - \epsilon(\gamma_i, \gamma_I))(1 - \epsilon(\gamma_2))$, where $1 - \epsilon(\gamma_i, \gamma_I)$ is the probability of decoding the message after retransmission and $\epsilon(\gamma_2)$ is the probability of decoding the fresh update with age $q = 1$ after removing the interference of the old update. Also, under action $a = 1$, if the sensor is unable to recover the fresh update then it can decode the old update due to retransmission with probability $(1 - \epsilon(\gamma_i, \gamma_I))\epsilon(\gamma_2)$. Since with each retransmission, the age increases with unit increment, if a status update is decoded after retransmission and the current status update fails, the system state would be $(2, 2)$. Finally, suppose the receiver is unable to recover the packet after the retransmission with action $a = 1$. In that case, it can only rely on the successfully recovered past packet, and the AoI increases from q to $q + 1$. The AoI would increase with retransmission and failing of the packet until the system reaches the maximum q upon which MDP truncate. We assume that if the receiver cannot decode the packet after retransmission, it does not attempt to recover the overlapping fresh update and considers it failed.

When the sensor takes action $a = 0$, the fresh update is available to the receiver with SNR P . Using N-CC-HARQ, when retransmission is requested, and the sensor takes action $a = 1$, the signal to interference and noise ratio (SINR) of the fresh update and the retransmitting old update vary with α . Because of the non-orthogonal transmission of old and fresh updates, the SINR for the retransmission of the old update is $\gamma_I = \frac{\alpha P}{1 + (1 - \alpha)P}$. Upon successfully decoding the retransmitting packet, its interference can be removed using SIC, and the receiver can attempt to decode the fresh update

with SNR $\gamma_2 = (1 - \alpha)P$. ■

The optimal policy can be obtained for N-CC-HARQ by associating the MSE cost function $\mathbb{C}(J_n, a) \triangleq \text{Tr}(f^q(\bar{\mathbf{P}}_0))$, to each state of the MDP process. Furthermore, the action sequence (policy) and choice of α provides distinct reliability versus age setting leading to more flexibility of AoI growth and optimal MSE performance. Under sufficient condition [11, Theorem 1], stationary and deterministic policy $\lambda(\alpha)$ exists that guarantees bounded long-term average MSE cost. Therefore for a given α , problem (18) is equivalent to the MDP average cost optimization problem. The MDP problem can be solved using standard methods such as relative value iteration algorithm [32]. The optimal policies corresponding to each discrete value of α can be compared to get the best $\lambda(\alpha)$ policy for outer optimization of problem (18). When the sensor does not change α with actions in each time slot, we refer to the policy as static-optimal policy. If the sensor can select α along with its action a in each time slot k , we refer to the policy as dynamic-optimal policy. The dynamic-optimal policy can utilize more flexibility, leading to further performance improvement. The dynamic-optimal policy is described in detail in the following.

D. Dynamic-optimal policy with N-CC-HARQ

If the sensor can select α in each time slot, it can provide more choice for packet reliability and AoI growth. Let $\alpha_k = \ell$ indicates sensor's selection of α in time slot k , where $\ell \in \{1, 2, \dots, L\}$ indicates L different choices of α . Therefore action $a = 0$ represents the action of sending a fresh packet with full power. Whereas, action $a = \ell$, corresponds to non-orthogonal retransmission with power-sharing fraction α_ℓ . The AoI update rule for N-CC-HARQ when α is varied dynamically under action $a = \ell$ is given as follows:

$$q_k(\ell) = \begin{cases} 1, & a_{k-1} = 0, \zeta_{k-1} = 0, \\ 1, & a_{k-1} = \ell, \zeta_{k-1}^o(\ell) = 0 \ \& \ \zeta_{k-1}^c = 0, \\ 2, & a_{k-1} = \ell, \zeta_{k-1}^o(\ell) = 0 \ \& \ \zeta_{k-1}^c(\ell) = 1, \\ q_{k-1}(\ell) + 1, & \zeta_{k-1} = 1 \ \text{or} \ \zeta_{k-1}^o(\ell) = 1. \end{cases} \quad (19)$$

Under N-CC-HARQ, packet length remains fixed; therefore, the AoI choices under dynamic setting look similar to the static case in (17). However, with dynamic selection of α_ℓ , the sensor can vary the packet failure rate between retransmitting old update and fresh update in each time slot. This leads to different available reliability and AoI setting with each ℓ . This key difference between static and dynamic settings allows more flexibility and reduces the AoI growth in each time slot. The policy optimization problem where the sensor can also choose α_ℓ for retransmission looks like.

$$\min_{\{a_1, a_2, \dots, a_k, \dots\} \forall a_k \in \mathbb{A}} \{\bar{\mu}_{\text{MSE}}, \rho_{\text{MSE}}\}, \quad (20)$$

where $\mathbb{A} \triangleq \{0, \ell\}$ and $\ell = [1, \dots, L]$.

We transform the optimization problem (20) to the equivalent MDP with state m_k and $q_k(\ell)$ for solving it numerically. The state space of the MDP problem is $\mathbb{J} \triangleq \{(m, q(\ell)) \in N \times N \times L\}$, where $J_k \triangleq (m_k, q_k(\ell)) \in \mathbb{J}$ is the state at k -

th time slot. Note that the dimension of state space increases according to the discrete choices of α_ℓ , i.e., maximum L . The action space $\mathbb{A} \triangleq \{0, \ell\}$, $\ell = [1, \dots, L]$ is defined by the action $a = 0$ and $a = \ell$, where action $a = \ell$ corresponds to the action of non-orthogonal retransmission with power sharing fraction α_ℓ . The state transition function $\mathbb{P}(J_n|J_c, a)$ of MDP for the dynamic setting is same as for the static case for $a = 0$ given in Lemma 1. The state transitions function for the dynamic case for $a = \ell$ is defined in Lemma 2.

Lemma 2. *When the sensor selects power sharing $a_k = \ell_1$ and $a_{k+1} = \ell_2$ in current and next time slot, respectively, the transition function $\mathbb{P}(J_n|J_c, a)$ between the current and next state is given as*

$$= \begin{cases} (1 - \epsilon(\gamma_i(\ell_1), \gamma_I(\ell_2))) (1 - \epsilon(\gamma_2(\ell_2))); & J_n = (1, 1), \\ (1 - \epsilon(\gamma_i(\ell_1), \gamma_I(\ell_2))) \epsilon(\gamma_2(\ell_2)); & J_n = (2, 2), \\ \epsilon(\gamma_i(\ell_1), \gamma_I(\ell_2)); & J_n = (2, q + 1), \\ 0; & \text{else,} \end{cases}$$

where $\gamma_1(\ell_1) = P$, $\gamma_2(\ell_1) = (1 - \alpha_{\ell_1})P$, $\gamma_2(\ell_2) = (1 - \alpha_{\ell_2})P$, $\gamma_I(\ell_2) = \frac{\alpha_{\ell_2}P}{1 + (1 - \alpha_{\ell_2})P}$, $\ell_1 = [0, 1, \dots, L]$ and $\ell_2 = [1, \dots, L]$.

Proof: The proof is similar to the proof of Lemma 1. The S(I)NRs variation between two time slots is due to dynamically selecting α_ℓ by the sensor in each time slot. With slight abuse of notation, $\ell_1 = 0$ value in $\ell = [0, 1, \dots, L]$ covers the case when action $a = 0$ is taken by the sensor in the current time slot. Therefore, $\alpha_0 = 0$ indicate this action of sending fresh update with full power, i.e., $\gamma_2(\ell_1 = 0) = (1 - \alpha_0)P = P$. ■

The instantaneous MSE cost is only the function of the AoI, i.e., $\mathbb{C}(J_n, a) \triangleq \text{Tr}(f^q(\bar{\mathbf{P}}_0))$. Using the standard relative value iteration algorithms for the MDP, the optimal policy is obtained that solves Problem (20).

IV. NUMERICAL RESULTS

In this section, we present simulation results for various optimal policies of HARQ enabled wireless networked control. We use MATLAB based MDP tool [34] to obtain the optimal policy using the relative value iteration algorithm. We use the following simulation parameters unless specified otherwise: The LTI system dynamics are set as $\mathbf{A} = [2.4, 0.2; 0.2, 0.8]$, $\mathbf{C} = [1, 1]$, $\mathbf{Q}_w = \mathbf{Q}_v = \mathbf{I}$ and $\rho^2(\mathbf{A}) = 1.8385^2$ and $\bar{\mathbf{P}}_0 = [2.5548, -1.6233; -1.6233, 1.6719]$. We set $\text{Tr}(\bar{\mathbf{P}}_0)$ as the MSE measure with single update at the beginning. All the simulations are conducted under AWGN channel conditions.

A. MSE versus the Delay optimal policies

It is assumed that reducing the delay leads to MSE minimization. However, by enabling HARQ based retransmissions, the packet reliability also increases, which helps in minimizing the MSE by recovering the failing packets with a slight increase in delay. We also show the performance of HARQ schemes under delay optimal policy. To obtain the optimal delay policy for any given HARQ scheme under action $a \in \{0, 1\}$, we change the cost function from MSE measure to AoI q . The long-term average age minimization problem is

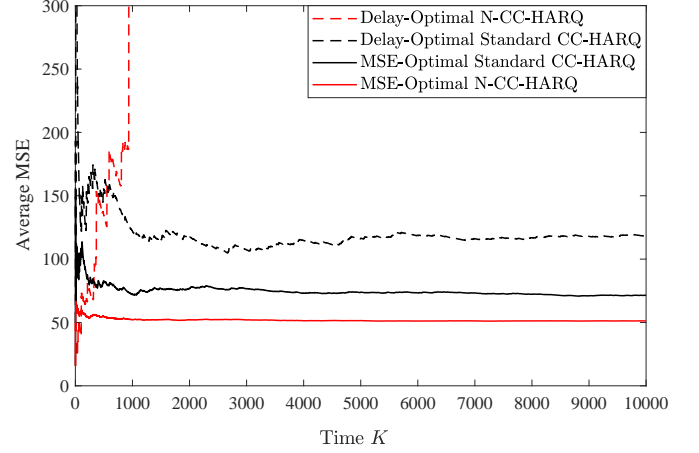


Fig. 4. Average MSE performance comparison between standard and proposed N-HARQ schemes under different optimal policies at SNR=0dB, $n = 100$, $k = 100$ and $\sigma^2(\mathbf{A}) = 2.4$

given as

$$\min_{\{a_1, a_2, \dots, a_k, \dots\}} \left\{ \lim_{K \rightarrow \infty} \frac{1}{K} \sum_{k=1}^K \mathbb{E}[q_k] \right\} \quad (21)$$

where for $a_k \in \{0, 1\}$ represent sensor's action of sending fresh update or a retransmission in time slot k . The optimal policy can be obtained using the corresponding MDP problem. The state space, action space and state transition function of the underlying MDP is similar to the MDP of MSE for any HARQ based scheme. Therefore, we omit its details here. However, the cost function of the MDP of the delay-optimal policy is the instantaneous AoI given as

$$c(m, q_k)|_{a_k = q_k}. \quad (22)$$

Using relative value iteration algorithm [32], the numerical solution of the MDP gives the delay-optimal policy that solves (21). MSE optimal policy is different than the delay (AoI) optimal policy because the cost and objective function is linear in terms of AoI (q). On the other hand, in the MSE optimal strategy, the cost function growth is non-linear with AoI.

In Fig. 4, we provide the long-term average MSE performance comparison between MSE-optimal and delay-optimal policies. We use standard CC-HARQ based optimal policy and static N-CC-HARQ based optimal policy corresponding to (18). The delay-optimal policy achieves poor MSE performance compared to MSE-optimal policy with both standard CC-HARQ and N-CC-HARQ schemes. Because MSE is a non-linear function of AoI (9) and slight increases in AoI leads to much worst MSE. With standard CC-HARQ, since the reliability is higher due to retransmission using full length and power, MSE growth is limited under the delay-optimal policy. With N-CC-HARQ, the MSE growth rate is very high due to inappropriate AoI minimization in each time slot under the delay-optimal policy. It is so much worst that it results in unbounded average MSE performance as shown Fig. 4. On the other hand, the MSE-optimal policy leads to much better performance with standard CC-HARQ and N-CC-HARQ. Therefore, in the following, we compare the optimal policies of the proposed IR-HARQ and CC-HARQ

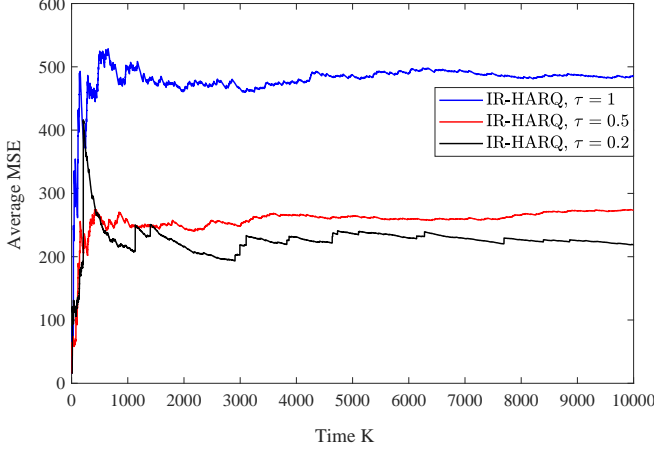


Fig. 5. Average MSE performance of IR-HARQ due to various retransmission coefficient τ at SNR=0dB when $n = k = 100$ and $\sigma^2(\mathbf{A}) = 4.4$

based schemes using MSE-optimal policies only.

B. IR-HARQ

First, we see the IR-HARQ schemes and performance of optimal-policy obtained by solving MDP problem corresponding to (14). The objective function of problem (14) consists of long-term average MSE and its standard deviation. The optimal policy $\lambda(\tau)$ achieves a particular MSE performance with a specific τ . In IR-HARQ, we find optimal policy under optimized retransmission parameter τ to achieve the best MSE performance. Fig. 5 presents the impact of τ on the long-term average MSE performance of IR-HARQ. As can be seen in Fig. 5, the smaller values of τ , e.g., 0.2 and 0.5, lead to a lower average MSE. Note that the IR-HARQ policy of [11] at $\tau = 1$ is sub-optimal as it sends the full retransmission and increases the AoI to the maximum with each retransmission. The age penalty due to retransmitting packets reduces with smaller τ . Fig. 5 indicates that the performance gain is higher by reducing τ from 1 to 0.5 than from 0.5 to 0.2. As τ reduces, the packet reliability also reduces. Therefore, shorter τ may cause consecutive packet failures in many time slots, especially when fewer retransmissions are allowed. In this situation, the AoI q and MSE grow much faster and more often, as seen in the form of higher fluctuations when $\tau = 0.2$ in Fig. 5. Therefore, the optimal τ that minimizes the standard deviation may not always be the lowest τ . Next, in Fig. 6, we show the impact of τ on the standard deviation of MSE which is the second objective function that relates to MSE stability in each time slot.

In real-time remote estimation, the packet-level performance is also important. In Fig. 6, we plot the distribution of the MSE performance in each time slot under the optimal policy at various τ settings. We test the performance of optimal policy by sending packets and drawing the MSE distribution using the Monte Carlo simulations for $K = 1000$ time slots. The MSE distribution shows the relative frequency of MSE variation at various τ settings. As can be seen in Fig. 6, the deviation of MSE from the mean is higher with $\tau = 0.2$ and $\tau = 1$ than $\tau = 0.5$. In real-time remote estimation, if

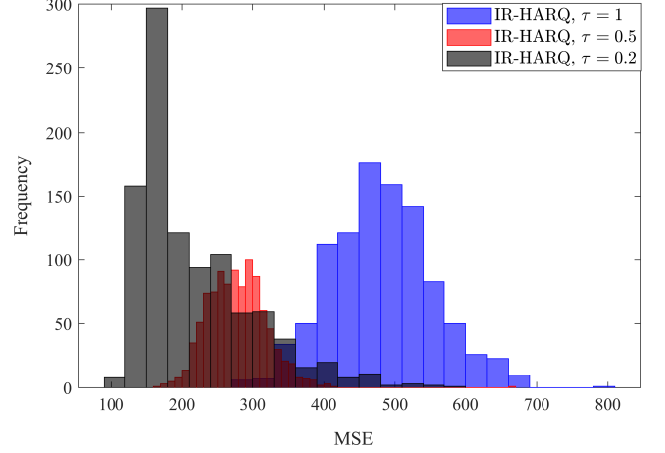


Fig. 6. MSE distribution of IR-HARQ due to various τ at SNR=0dB and $n = k = 100$ and $\sigma^2(\mathbf{A}) = 4.4$.

a packet fails, the receiver estimates the current state using the last successful update with higher AoI q . At $\tau = 0.2$, HARQ retransmissions provide very low reliability to failing packets, and erroneous packets are mostly not recovered after the retransmission. Therefore, MSE deviates significantly from the mean with higher frequency in each time slot as shown in Fig. 6, for $\tau = 0.2$. On the other hand, the setting $\tau = 1$ gives reliability more than required at the cost of higher AoI in each time slot due to retransmission. More specifically, each retransmission at $\tau = 1$ causes the MSE performance penalty leading to an overall higher MSE deviation from the average MSE performance as shown in Fig. 6, for $\tau = 1$. The setting $\tau = 0.5$ provides required reliability with the lowest possible AoI growth with each retransmission. Finally, the optimal policy with $\tau = 0.5$ would be selected to get optimal performance for the optimization (14). Therefore, among the settings $\tau = 0.2$, $\tau = 0.5$ and $\tau = 1$, the setting $\tau = 0.5$ is the best choice for long-term average MSE over many time slots and more stable MSE performance in each time slot.

C. CC-HARQ

Next, we present the MSE performance of the proposed N-CC-HARQ scheme under static-optimal policy corresponding to (18).

In Fig. 7, we compare the MSE performance of standard CC-HARQ with N-CC-HARQ. The standard CC-HARQ retransmits the old update in the entire time slot. In contrast, N-CC-HARQ conducts retransmission using power-sharing parameter α to update current status along with retransmission of old update. We show the effect of selecting different α on the long-term average MSE performance of N-CC-HARQ in Fig. 7. As can be seen in this figure, with N-CC-HARQ, $\alpha = 0.1$ achieves the best long-term average MSE performance followed by the setting $\alpha = 0.9$, while $\alpha = 0.4$ gives the worst performance. This is because at setting $\alpha = 0.1$ and 0.9, the power difference between non-orthogonal packet is higher which leads to better decoding under SIC. When the overlapping packets are at similar power levels, e.g., $\alpha = 0.4$, it is challenging to separate non-orthogonal packets

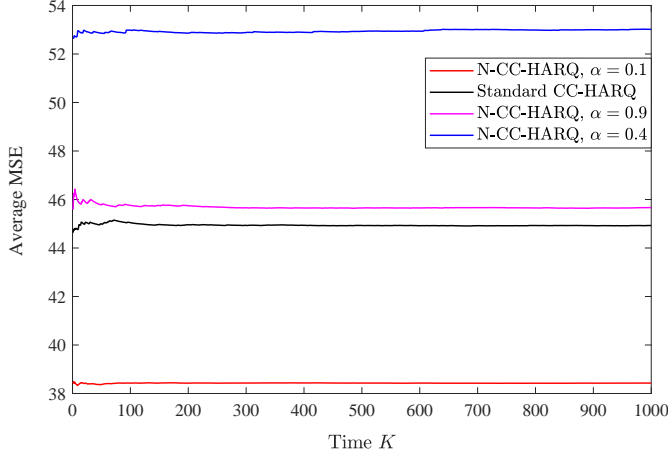


Fig. 7. Average MSE performance of N-CC-HARQ with static-optimal policy due to various α at SNR=0dB and $n = k = 100$ and $\sigma^2(\mathbf{A}) = 2.0$.

successfully using SIC. Comparing $\alpha = 0.1$ and $\alpha = 0.9$, the setting $\alpha = 0.9$ assigns excessive power for sending old updates, which leaves less power for fresh status updates and causes estimation errors. The standard CC-HARQ also suffers from poor MSE performance due to excessive retransmission overhead. Since at $\sigma^2(\mathbf{A}) = 2.0$, the correlation between status updates is higher and fresh updates with a little higher reliability is more suitable. At $\alpha = 0.1$, the non-orthogonal fresh updates are decoded with good reliability while utilizing enough retransmissions to save failing old updates. Therefore, under given packet reliability and process correlation profile, i.e., $\sigma^2(\mathbf{A}) = 2.0$, the optimal policy with $\alpha = 0.1$ achieves the best long-term average MSE performance.

The histogram of MSE in Fig. 8 depicts the standard deviation of MSE given in (11) due to static-optimal policy $\lambda(\alpha)$ corresponding to N-CC-HARQ (18) at various α . In Fig. 8, we show the MSE performance comparison between standard CC-HARQ and N-CC-HARQ. At $\alpha = 0.4$, the policy leads to unstable MSE performance, primarily due to inaccurate SIC decoding of N-CC-HARQ. The packet failure rate is reduced by increasing the retransmission power from $\alpha = 0.4$ to $\alpha = 0.9$. However, at $\alpha = 0.9$, the retransmission power is excessive, and the overlapping fresh update is transmitted with less power ($1 - \alpha = 0.1$) which would require a retransmission. Excessive retransmissions over many time slots increase the AoI and lead to sub-optimal and unstable MSE performance, as can be seen in Fig. 8, for $\alpha = 0.9$. The MSE variation of standard CC-HARQ is almost similar to N-CC-HARQ at $\alpha = 0.9$ because of roughly the same power assignment to send old updates considering the correlation of the dynamic process $\sigma^2(\mathbf{A}) = 2.0$. At $\alpha = 0.1$ sensor uses the exact required power to conduct retransmission leaving enough power to send fresh update. This results in more packets being decoded successfully in consecutive time slots leading to better and more stable MSE performance.

The eigenvalue $\sigma^2(\mathbf{A})$ of the LTI system matrix represents the correlation of the dynamic process under observation through the sensors. The $\sigma^2(\mathbf{A}) = 2.4$ indicates that the process is changing slowly per time slot and estimation quality degrades slowly with AoI. The controller can predict the

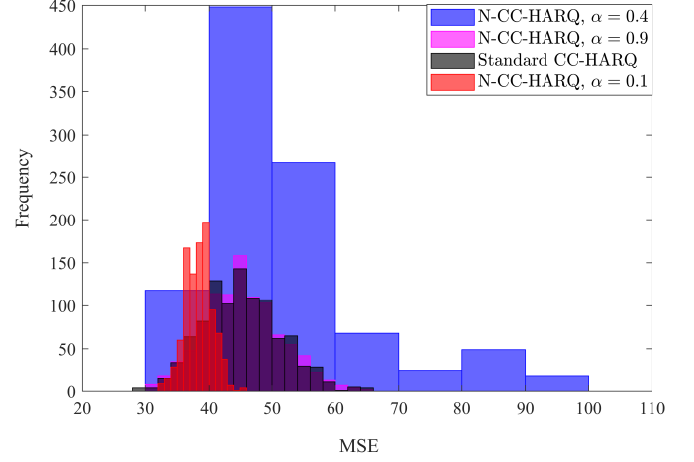


Fig. 8. MSE distribution of N-CC-HARQ due to various α and standard CC-HARQ at SNR=0dB when $n = k = 100$ and $\sigma^2(\mathbf{A}) = 2.0$.

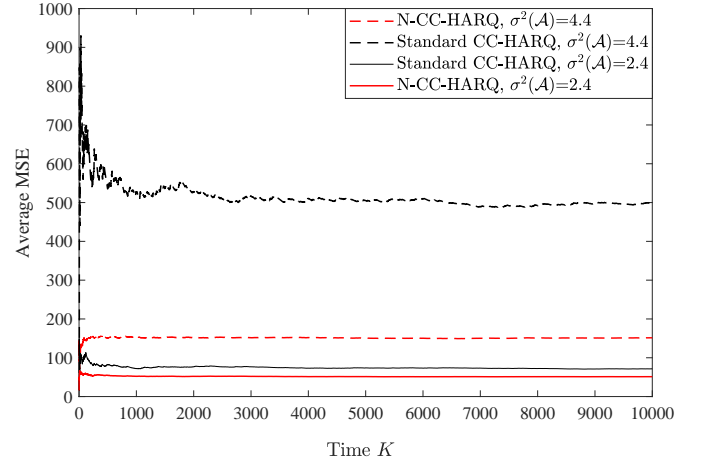


Fig. 9. Average MSE performance comparison of optimal policy with standard CC-HARQ and static-optimal policy using N-CC-HARQ with $\alpha = 0.1$ in AWGN for different $\sigma^2(\mathbf{A})$ at $n = k = 100$ and SNR=0dB when $m = 2$.

current update from the old update with less estimation error during packet loss. Therefore, the performance gap between standard CC-HARQ and N-CC-HARQ is small. Conversely, at $\sigma^2(\mathbf{A}) = 4.4$, the cost penalty is higher with increasing AoI. Therefore, a longer packet for retransmission can deteriorate the MSE estimation performance. For N-CC-HARQ, we select $\alpha = 0.1$ to minimize long-term average MSE. Fig. 9 shows that N-CC-HARQ is more effective in limiting MSE cost penalty as it offers more flexibility of selecting reliability and AoI points. Standard CC-HARQ takes a retransmission action with full power and time slot utilization, which increases the AoI especially when correlation is low. Therefore, the performance gap between N-CC-HARQ and standard CC-HARQ schemes further increases at $\sigma^2(\mathbf{A}) = 4.4$, when estimation error increases rapidly with AoI.

In Fig. 10, we compare the MSE performance of N-CC-HARQ with the dynamic-optimal and static-optimal policies. Under the dynamic-optimal policy, the sensor can vary α_ℓ in each time slot as given in (20). Therefore, the sensor chooses the best action in each time slot that leads to further

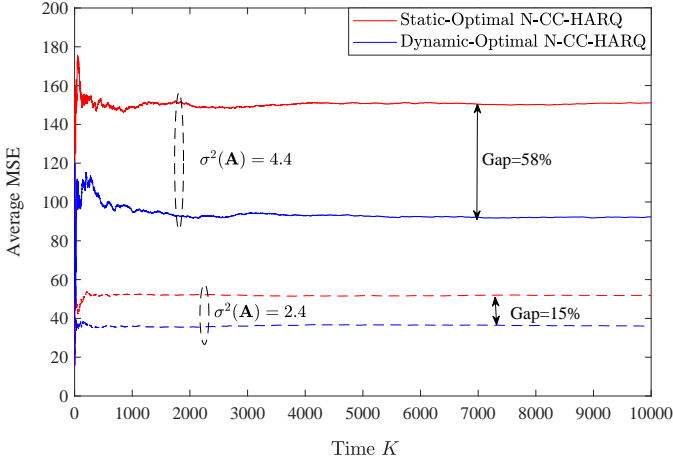


Fig. 10. Average MSE performance of static-optimal N-CC-HARQ with $\alpha = 0.1$ and dynamic-optimal N-CC-HARQ with $L = 11$ power levels, i.e., $\alpha_\ell \in \{0, 0.1, 0.2, \dots, 1\}$ in AWGN channel at $n = k = 100$, SNR=0dB and $m = 2$

performance improvements, as evident in Fig. 10. For example, suppose sensor allocates higher α for retransmission of old update at time slot $k - 1$. It can reduce its impact by allocating more retransmission power for retransmission of the following status update; leading to more controlled growth of AoI. More specifically, when the AoI is low, the sensor chooses a smaller value of α_ℓ , i.e., $\{0, 0.1, \dots, 0.5\}$ for AoI $\{1, 2, \dots, 6\}$ respectively. When AoI is higher due to consecutive packet failure, the sensor selects higher power levels such as 0.9 and 1 to limit the AoI growth. The dynamic-optimal policy structure depends upon operating SNR, rate, and $\sigma^2(\mathbf{A})$. Under the dynamic-optimal policy, N-CC-HARQ gives 15% performance improvements over the static-optimal policy to minimize long-term average MSE when $\sigma^2(\mathbf{A}) = 2.4$. Furthermore, when the correlation between status updates is low, i.e., $\sigma^2(\mathbf{A}) = 4.4$, the MSE gain of dynamic policy over static is increased with a 58% gain. Each power fraction α_ℓ corresponds to a specific packet reliability versus AoI setting. Dynamically selecting α gives the sensor the flexibility to choose suitable reliability during retransmission in each time slot. On the other hand, in static N-CC-HARQ the choice of α_ℓ remains fixed associated with specific reliability versus AoI growth. In this way, the dynamic setting becomes more general, while static optimization is one instance of the dynamic strategy.

Fig. 11 shows the histograms of the MSE for various CC-HARQ schemes under corresponding optimal policies. For real-time control systems, the instantaneous estimation MSE is also as important as its long-term average MSE. The policy with higher MSE variance can lead to instability in the control process. Fig. 11 shows the MSE distribution, where the approach that attains a smaller deviation from the mean MSE is more stable. The performance of optimal policy with standard CC-HARQ performs worst in providing stable and low MSE. This is because standard CC-HARQ increases packet reliability with maximum increases in AoI, leading to poor and highly unstable MSE performance. The proposed N-CC-HARQ can avoid that by adjusting the AoI growth using an additional variable α . The static-optimal policy with N-

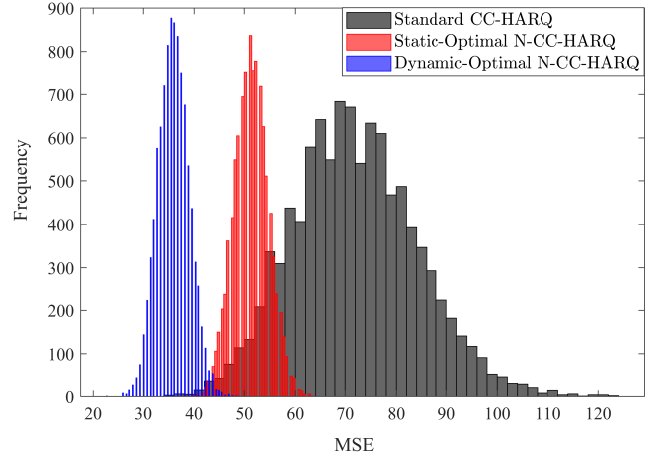


Fig. 11. MSE distributions of standard CC-HARQ, static-optimal N-CC-HARQ with $\alpha = 0.1$ and dynamic-optimal N-CC-HARQ with $L = 11$ power levels, i.e., $\alpha_\ell \in \{0, 0.1, 0.2, \dots, 1\}$ in AWGN channel at $n = k = 100$, SNR=0dB and $m = 2$

CC-HARQ reduces the MSE and provides more controlled MSE growth in each time slot. Furthermore, the dynamic-optimal policy based on N-CC-HARQ can further limit the MSE deviation compared to the static-optimal policy for N-CC-HARQ. This is due to a higher level of control over AoI growth with retransmissions in each time slot.

V. PRACTICAL CONSIDERATIONS

For HARQ based MDP, since AoI increases with each packet failure, therefore it can have infinitely many states. However, we truncate it to some finite value for offline numerical evaluation. For example, we use state-space truncation with maximum single retransmission and the AoI growth to a maximum number N . The standard HARQ based schemes involve a $2N \times 2N$ dimensional state transition matrix with each action. The computation complexity of policies in the standard HARQ case is $\mathcal{O}(2N^2K)$ [35]. In the proposed IR-HARQ with fractional growth of q with τ_ℓ the state transition probability matrix has dimension $2N\tau_\ell^{-1} \times 2N\tau_\ell^{-1}$. L such MDP problems are solved to select the best τ_ℓ for the optimal policy. The dimension of the state transition matrix for CC-HARQ and N-CC-HARQ remains fixed due to fixed points of AoI q growth. However, the complexity of N-CC-HARQ MDP is higher due to additional optimization over α_ℓ . Note that the additional SIC computing complexity of N-CC-HARQ can increase the delay. But this can be avoided using parallel computing for standard non-orthogonal HARQ schemes. However, the dynamic non-orthogonal HARQ schemes suffer from slow convergence due to high complexity.

Furthermore, additional feedback signaling is required to implement the optimal policy using a non-orthogonal HARQ procedure. Because more updates are sent per time slot using non-orthogonal signaling. Also, the dynamic-optimal strategy has higher complexity as action space is large, and the sensor can select different α_ℓ in different time slots. This requires higher bits for feedback control signaling to update the value of α_ℓ as it changes for proper SIC decoding.

VI. CONCLUSION

We proposed wireless network control for remote estimation of the LTI dynamical systems under various IR-HARQ and CC-HARQ based packet retransmission schemes. For IR-HARQ, optimized retransmission improved the MSE performance due to the early arrival of fresh status updates. We optimized the standard CC-HARQ schemes and allowed non-orthogonal retransmissions that increases the packet reliability gradually and limited the AoI growth. The power-sharing fraction α is optimized for the sensor policy under non-orthogonal CC-HARQ scheme. The static-optimal policy, when α remained fixed in many time slots, improved the MSE performance compared to the optimal policy with standard CC-HARQ. We also presented the dynamic-optimal policy that enhanced the MSE performance significantly. We used the Markov decision process formulation to solve complex optimization problems and obtain optimal policies using numerical techniques. Simulation results exhibited significantly better long-term average and packet-level MSE performance using the proposed optimal policies over standard HARQ based optimal policies.

REFERENCES

- [1] G. Varrall, *5G spectrum and standards*. Artech House, 2016.
- [2] K. Antonakoglou, X. Xu, E. Steinbach, T. Mahmoodi, and M. Dohler, "Toward haptic communications over the 5G tactile Internet," *IEEE Communications Surveys & Tutorials*, vol. 20, no. 4, pp. 3034–3059, 2018.
- [3] C. Peng and T. C. Yang, "Event-triggered communication and control co-design for networked control systems," *Automatica*, vol. 49, no. 5, pp. 1326–1332, 2013.
- [4] F. Peng, Z. Jiang, S. Zhou, Z. Niu, and S. Zhang, "Sensing and communication co-design for status update in multiaccess wireless networks," *IEEE Transactions on Mobile Computing*, 2021.
- [5] M. Bennis, M. Debbah, and H. V. Poor, "Ultrareliable and low-latency wireless communication: Tail, risk, and scale," *Proceedings of the IEEE*, vol. 106, no. 10, pp. 1834–1853, 2018.
- [6] R. D. Yates, Y. Sun, D. R. Brown, S. K. Kaul, E. Modiano, and S. Ulukus, "Age of information: An introduction and survey," *IEEE Journal on Selected Areas in Communications*, vol. 39, no. 5, pp. 1183–1210, 2021.
- [7] T. Z. Ornee and Y. Sun, "Sampling and remote estimation for the ornstein-uhlenbeck process through queues: Age of information and beyond," *IEEE/ACM Transactions on Networking*, 2021.
- [8] S. Roth, A. Arafa, H. V. Poor, and A. Sezgin, "Remote short blocklength process monitoring: Trade-off between resolution and data freshness," in *ICC 2020-2020 IEEE International Conference on Communications (ICC)*. IEEE, 2020, pp. 1–6.
- [9] N. Rajaraman, R. Vaze, and G. Reddy, "Not just age but age and quality of information," *IEEE Journal on Selected Areas in Communications*, vol. 39, pp. 1325–1338, 2021.
- [10] Z. Wang, M.-A. Badiu, and J. P. Coon, "A value of information framework for latent variable models," in *GLOBECOM 2020-2020 IEEE Global Communications Conference*. IEEE, 2020, pp. 1–6.
- [11] K. Huang, W. Liu, M. Shirvanimoghaddam, Y. Li, and B. Vucetic, "Real-time remote estimation with hybrid ARQ in wireless networked control," *IEEE Transactions on Wireless Communications*, vol. 19, no. 5, pp. 3490–3504, 2020.
- [12] E. T. Ceran, D. Gündüz, and A. György, "Average age of information with hybrid ARQ under a resource constraint," *IEEE Transactions on Wireless Communications*, vol. 18, no. 3, pp. 1900–1913, 2019.
- [13] K. Huang, W. Liu, Y. Li, and B. Vucetic, "To retransmit or not: Real-time remote estimation in wireless networked control," in *ICC 2019-2019 IEEE International Conference on Communications (ICC)*. IEEE, 2019, pp. 1–7.
- [14] S. Asvadi, S. Fardi, and F. Ashtiani, "Analysis of peak age of information in blocking and preemptive queueing policies in a harq-based wireless link," *IEEE Wireless Communications Letters*, vol. 9, no. 9, pp. 1338–1341, 2020.
- [15] F. Nadeem, Y. Li, B. Vucetic, and M. Shirvanimoghaddam, "Analysis and optimization of HARQ for URLLC," *arXiv preprint arXiv:2110.02163*, 2021.
- [16] B. Zhang, L. B. Milstein, and P. Cosman, "Energy optimization for hybrid ARQ with turbo coding: Rate adaptation and allocation," *IEEE Transactions on Vehicular Technology*, vol. 69, no. 10, pp. 11 338–11 352, 2020.
- [17] "3GPP TR 38.824 Study on physical layer enhancements for NR ultra-reliable low latency communication (URLLC) (Release 16)," 3rd Generation Partnership Project, Technical Specification Group Radio Access Network, Tech. Rep., Oct. 2018.
- [18] F. Nadeem, M. Shirvanimoghaddam, Y. Li, and B. Vucetic, "Delay-sensitive NOMA-HARQ for short packet communications," *Entropy*, vol. 1, no. 0, pp. 000–000, 2021.
- [19] —, "Non-orthogonal HARQ for URLLC: Design and analysis," *IEEE Internet of Things Journal*, 2021.
- [20] M. Shirvanimoghaddam, H. Khayami, Y. Li, and B. Vucetic, "Dynamic HARQ with guaranteed delay," in *2020 IEEE Wireless Communications and Networking Conference (WCNC)*. IEEE, 2020, pp. 1–6.
- [21] L. Schenato, "Optimal estimation in networked control systems subject to random delay and packet drop," *IEEE transactions on automatic control*, vol. 53, no. 5, pp. 1311–1317, 2008.
- [22] W. Liu, X. Zhou, S. Durrani, H. Mehrpouyan, and S. D. Blostein, "Energy harvesting wireless sensor networks: Delay analysis considering energy costs of sensing and transmission," *IEEE Transactions on Wireless Communications*, vol. 15, no. 7, pp. 4635–4650, 2016.
- [23] L. Shi and H. Zhang, "Scheduling two Gauss-Markov systems: An optimal solution for remote state estimation under bandwidth constraint," *IEEE Transactions on Signal Processing*, vol. 60, no. 4, pp. 2038–2042, 2012.
- [24] P. S. Maybeck, *Stochastic models, estimation, and control*. Academic press, 1982.
- [25] M. B. Rhudy and Y. Gu, "Online stochastic convergence analysis of the kalman filter," *International Journal of Stochastic Analysis*, 2013.
- [26] Y. Polyanskiy, H. V. Poor, and S. Verdú, "Channel coding rate in the finite blocklength regime," *IEEE Transactions on Information Theory*, vol. 56, no. 5, p. 2307, 2010.
- [27] C. Sahin, L. Liu, E. Perrins, and L. Ma, "Delay-sensitive communications over IR-HARQ: Modulation, coding latency, and reliability," *IEEE Journal on Selected Areas in Communications*, vol. 37, no. 4, pp. 749–764, 2019.
- [28] T. Erseghe, "Coding in the finite-blocklength regime: Bounds based on laplace integrals and their asymptotic approximations," *IEEE Transactions on Information Theory*, vol. 62, no. 12, pp. 6854–6883, 2016.
- [29] F. Nadeem, M. Shirvanimoghaddam, Y. Li, and B. Vucetic, "Non-orthogonal HARQ for delay sensitive applications," in *IEEE International Conference on Communications (ICC)*. IEEE, 2020, pp. 1–6.
- [30] S. Kaul, R. Yates, and M. Gruteser, "Real-time status: How often should one update?" in *2012 Proceedings IEEE INFOCOM*. IEEE, 2012, pp. 2731–2735.
- [31] S. Wu, K. Ding, P. Cheng, and L. Shi, "Optimal scheduling of multiple sensors over lossy and bandwidth limited channels," *IEEE Transactions on Control of Network Systems*, vol. 7, no. 3, pp. 1188–1200, 2020.
- [32] M. L. Littman, T. L. Dean, and L. P. Kaelbling, "On the complexity of solving markov decision problems," *arXiv preprint arXiv:1302.4971*, 2013.
- [33] K. Huang, W. Liu, Y. Li, A. Savkin, and B. Vucetic, "Wireless feedback control with variable packet length for industrial IoT," *IEEE Wireless Communications Letters*, vol. 9, no. 9, pp. 1586–1590, 2020.
- [34] M.-J. Cros, "Markov decision process (MDP) toolbox for MATLAB," *MATLAB Central file exchange*, Retrieved: 2020, [Online] Available: (<https://au.mathworks.com/matlabcentral/fileexchange/25786-markov-decision-processes-mdp-toolbox>).
- [35] L. I. Sennott, *Stochastic dynamic programming and the control of queueing systems*. John Wiley & Sons, 2009, vol. 504.